C^1 Hermite interpolations with RPH curves

Hyun Chol Lee[a], Jae Won Lee[a], Dae Won Yoon[a,*]

[a]Department of Mathematics Education and RINS, Gyeongsang National University, Jinju 52828, Republic of Korea

Abstract. In this paper, we study C^1 Hermite interpolation with a spatial rational Pythagorean hodograph (RPH) curve for a regular C^1 Hermite data set. In particular, we completely classify simple PH Möbius cubics and prove that there exist two scaled Enneper surfaces as a PH-preserving mapping satisfying the given C^1 Hermite data set. Also, we give the algorithm to construct RPH curves on the Enneper surface by using PH Möbius cubics and scaled PH-preserving mappings. Finally, we calculate arc-length and bending energy of these RPH curves to choice the best RPH curves on the Enneper surface, and give some examples for RPH curves.

1. Introduction

Computer Aided Design (CAD) and Computer Aided Manufacturing (CAM) system mostly respond to Non-Uniform Rational B-Spline (NURBS) representations of curves and surfaces, given by polynomial or rational parameterizations. A natural question is to have offset curves and surfaces represented by rational parameterizations. However, the rationality of these both curves and surfaces is not generally preserved. To study special classes of curves and surfaces with rational offsets, Farouki and Sakkalis [6] introduced firstly a Pythagorean Hodograph (PH) curve, which is the planar polynomial curve with a polynomial speed function. The most significant properties of these curves offer a polynomial arc length, a rational curvature and a rational offset curve.

Later, the concept of polynomial planar PH curves is extended to spatial polynomial PH curves [4, 9], to planar rational PH curves [16], and to spatial rational PH curves [8, 14] in Euclidean space. Such PH curves are used in mechanical engineering and interpolation of discrete data control of motion along curved paths, and the related results for practical applications of PH curves are shown in [1, 3, 7, 13, 16–18]. Also, PH curves have been generalized to participate in the medial axis transform defined by the set of the centers of the maximal inscribed disks, becoming Minkowski PH (MPH) curves in the three dimensional Minkowski space [5, 15]. For the results of MPH curves, we refer to [2, 10, 11]

The paper is arranged as follows: In Section 2, after briefly reviewing some fundamental definitions of a PH curve and a C^1 Hermite data set, we clarify the existence of simple PH Möbius cubics. In Section 3, we

show that a parametrization of the Enneper surface is PH-preserving, and also there are two scaled Enneper surfaces satisfying any regular C^1 Hermite data set. Also, we construct spatial RPH curves satisfying the C^1 Hermite data set on the Enneper surfaces. Moreover, we introduce how to compute the bending energy for curves on the surface in order to choose better curves as well as we analyze arc length and bending energy through examples.

2. PH Möbius cubics

Let $\mathbb{R}^n$ be the n-dimensional Euclidean space and let $\mathbb{R}(t)$ be the set of rational functions with real coefficients. We express a rational curve in $\mathbb{R}^n$ as a mapping $\mathbf{r}: \mathbb{R} \to \mathbb{R}^n$, via $t \mapsto (x_1(t), x_2(t), \dots, x_n(t))$, $x_i(t) \in \mathbb{R}(t)$ $(1 \le i \le n)$.

Definition 2.1. A rational curve $\mathbf{r}(t) = (x_1(t), x_2(t), \dots, x_n(t))$ is said to be a *rational Pythagorean-hodograph (RPH) curve* if its velocity vector or hodograph $\mathbf{r}'(t) = (x_1'(t), \dots x_n'(t))$ satisfies the Pythagorean condition;

$$\exists\, \sigma(t) \in \mathbb{R}(t) \text{ such that } \|\mathbf{r}'(t)\|^2 = x_1'(t)^2 + x_2'(t)^2 + \cdots + x_n'(t)^2 = \sigma(t)^2.$$

Now, we introduce PH Möbius cubics as planar RPH curves satisfying a C^1 Hermite data set.

Let $\mathbf{P}_0$ and $\mathbf{P}_1$ be the initial and final points in $\mathbb{R}^2$(or $\mathbb{C}$) to be interpolated with $\mathbf{P}_0 \ne \mathbf{P}_1$. Let $\mathbf{V}_0$ and $\mathbf{V}_1$ be the initial vector at $\mathbf{P}_0$ and the final vector at $\mathbf{P}_1$, respectively. In this case, a set $H^2_{C^1} = \{\mathbf{P}_0, \mathbf{P}_1, \mathbf{V}_0, \mathbf{V}_1\}$ is called a C^1 *Hermite data set*. In particular, by an appropriate rigid motion we can arrange as $\mathbf{P}_0 = 0$ and $\mathbf{P}_1 = 1$, a set $\{0, 1, \mathbf{V}_0, \mathbf{V}_1\}$ is called a *standard C^1 Hermite date set* and denoted by $\tilde{H}^2_{C^1}$.

Consider a planar PH curve $\mathbf{r}(t)$ $(0 \le t \le 1)$ and a Möbius transformation $\Phi(\mathbf{z}) = \frac{a\mathbf{z}+b}{c\mathbf{z}+d}$ in the extended complex plane $\mathbb{C}_\infty = \mathbb{C} \cup \{\infty\}$ for some complex numbers a, b, c, d with $ad - bc \ne 0$. We known that $(\Phi \circ \mathbf{r})(t)$ is a RPH curve [12]. If $\mathbf{r}(t)$ is a PH cubic then $(\Phi \circ \mathbf{r})(t)$ is called a *PH Möbius cubic*. Suppose that a RPH curve $(\Phi \circ \mathbf{r})(t)$ satisfies the standard C^1 Hermite data set $\tilde{H}^2_{C^1}$. Then one yields

$$\begin{aligned} (\Phi \circ \mathbf{r})(0) &= 0, \quad \int_0^1 (\Phi \circ \mathbf{r})'(t)\, dt = 1, \\ (\Phi \circ \mathbf{r})'(0) &= \mathbf{V}_0, \quad (\Phi \circ \mathbf{r})'(1) = \mathbf{V}_1. \end{aligned} \tag{2.1}$$

From these conditions, we have the following theorem:

Theorem 2.2. *For a given standard C^1 Hermite data set $\tilde{H}^2_{C^1} = \{0, 1, \mathbf{V}_0, \mathbf{V}_1\}$ with $\mathbf{V}_0\mathbf{V}_1 \notin \mathbb{R}^+$, there are PH Möbius cubics satisfying the set $\tilde{H}^2_{C^1}$.*

Proof. Consider a Möbius transformation $\Phi(\mathbf{z}) = \frac{\alpha \mathbf{z}}{(\alpha-1)\mathbf{z}+1}$ and a PH cubic $\mathbf{r}(t) = \mathbf{k}(t - \mathbf{c})^3 + \mathbf{d}$, where $\alpha, \mathbf{k} \in \mathbb{C}^*$, $\mathbf{c} \in \mathbb{C}/\mathbb{R}$, $\mathbf{d} \in \mathbb{C}$. From (2.1), the PH cubic $\mathbf{r}(t)$ satisfies

$$\mathbf{r}(0) = 0, \quad \int_0^1 \mathbf{r}'(t)\, dt = 1, \quad \mathbf{r}'(0) = \frac{1}{\alpha}\mathbf{V}_0, \quad \mathbf{r}'(1) = \alpha\mathbf{V}_1, \tag{2.2}$$

which imply

$$\begin{aligned} \mathbf{r}(1) - \mathbf{r}(0) &= \mathbf{k}(1 - 3\mathbf{c} + 3\mathbf{c}^2) = 1, \\ \mathbf{r}'(0) &= 3\mathbf{k}\mathbf{c}^2 = \frac{\mathbf{V}_0}{\alpha}, \\ \mathbf{r}'(1) &= 3\mathbf{k}(1 - \mathbf{c})^2 = \alpha\mathbf{V}_1. \end{aligned} \tag{2.3}$$

Eliminating α and $\mathbf{k}$ in (2.3), we have

$$\mathbf{V}_0\mathbf{V}_1(3\mathbf{c}^2 - 3\mathbf{c} + 1)^2 = 9(\mathbf{c}^2 - \mathbf{c})^2. \tag{2.4}$$

Let $A = 3\mathbf{c}^2 - 3\mathbf{c}$. Then equation (2.4) can be rewritten as

$$A = \frac{1}{-1 \pm \omega},\tag{2.5}$$

where $\omega = \sqrt{\frac{1}{\mathbf{V}_0 \mathbf{V}_1}}$. Solving the quadratic equation (2.5), we obtain

$$\mathbf{c} = \frac{1}{2}\left(1 \pm \sqrt{1 + \frac{4}{3\,(-1 \pm \omega)}}\right).\tag{2.6}$$

Since $\mathbf{V}_0 \mathbf{V}_1 \notin \mathbb{R}^+$, $\mathbf{c} \in \mathbb{C}/\mathbb{R}$. Consequently, we can find four distinct PH Möbius cubic interpolants satisfying the standard C^1 Hermite data set $\tilde{H}^2_{C^1}$ according to the complex number $\mathbf{c}$. Thus, this completes the proof. $\square$

Note that if $\mathbf{V}_0 \mathbf{V}_1 \in \mathbb{R}^+$, we need additional explanation about the possibility of PH Möbius cubic interpolants according to $\mathbf{c}$ in (2.6), and we give the classification for PH Möbius cubics in the following theorem.

Theorem 2.3. *If $\mathbf{V}_0 \mathbf{V}_1 \in \mathbb{R}^+$, we can classify all the possible PH Möbius cubic interpolants as follows:*

(1) *If $\mathbf{V}_0 \mathbf{V}_1 > 9$, then $1 + \frac{4}{3(-1+\omega)} < 0$ and $1 + \frac{4}{3(-1-\omega)} < 0$. Therefore there exist four distinct PH Möbius cubic interpolants.*

(2) *If $1 < \mathbf{V}_0 \mathbf{V}_1 \le 9$, then $1 + \frac{4}{3(-1+\omega)} < 0$ and $1 + \frac{4}{3(-1-\omega)} \ge 0$. Therefore there exist two distinct PH Möbius cubic interpolants.*

(3) *If $0 < \mathbf{V}_0 \mathbf{V}_1 \le 1$ and $\mathbf{c} \in \mathbb{R}$, there exist no any PH Möbius cubic interpolants.*

Furthermore, since a Möbius transformation is a one-to-one correspondence on the extended complex plane $\mathbb{C}_\infty = \mathbb{C} \cup \{\infty\}$, we can determine whether the interpolate of a PH Möbius cubic is a loop as the following lemma.

Lemma 2.4. *Let $\mathbf{r}(t) = \int_0^t \mathbf{k}(\tau - \mathbf{c})^2 d\tau + \mathbf{r}(0)$ be a PH cubic. Then $\mathbf{r}(t)$ has a loop if and only if $\mathbf{c} \in \Omega_1 \cup \Omega_2$, where*

$$\Omega_1 = \{z \in \mathbb{C} \mid 0 \le \mathrm{Re}(z) - \sqrt{3}\,\mathrm{Im}(z) < \mathrm{Re}(z) + \sqrt{3}\,\mathrm{Im}(z) \le 1\}$$

and

$$\Omega_2 = \{z \in \mathbb{C} \mid 0 \le \mathrm{Re}(z) + \sqrt{3}\,\mathrm{Im}(z) < \mathrm{Re}(z) - \sqrt{3}\,\mathrm{Im}(z) \le 1\}$$

shown in Figure 1(a).

In Theorem 2.2, let $A(\mathbf{z}) = 3\mathbf{z}^2 - 3\mathbf{z}$. Then we have $A(\Omega_1) = A(\Omega_2)$. Since $-1 + \omega$ and $-1 - \omega$ are mutually symmetric at the point $-1 + 0\,i$, one of $\frac{1}{-1+\omega}$ and $\frac{1}{-1-\omega}$ belongs to the circle $D = \{z \in \mathbb{C} : |z| = 1\}$ and the other is not in D. Also, in (2.6), letting $v = \frac{1}{2}\sqrt{1 + \frac{4}{3(-1\pm\omega)}}$, $\mathbf{c} = \frac{1}{2} + v$ and $\mathbf{c} = \frac{1}{2} - v$ are symmetric each other at the point $\frac{1}{2} + 0\,i$. On Ω_1 and Ω_2, $\frac{1}{2} + v$ and $\frac{1}{2} - v$ are thus all simple curves or all loops (see Figure 1.(b)). Consequently, we obtain the following theorem.

Theorem 2.5. *For a given standard C^1 Hermite data set $\tilde{H}^2_{C^1} = \{0, 1, \mathbf{V}_0, \mathbf{V}_1\}$, the following statements are hold for PH Möbius cubics:*

(1) *If $\mathbf{V}_0 \mathbf{V}_1 \in \mathbb{C} /\{x \in \mathbb{R} : 0 \le x < 9\}$, there are at least two simple PH Möbius cubic interpolants.*

(2) *If $1 < \mathbf{V}_0 \mathbf{V}_1 \le 9$, two interpolants are all simple curves or all loops.*

Remark 2.6. *For a given standard C^1 Hermite data set $\tilde{H}^2_{C^1} = \{0, 1, \mathbf{V}_0, \mathbf{V}_1\}$ with $\mathbf{V}_0 \mathbf{V}_1 \notin \{x \in \mathbb{R} : 0 \le x \le 9\}$, there exist simple PH Möbius cubic interpolants satisfying the set $\tilde{H}^2_{C^1}$.*

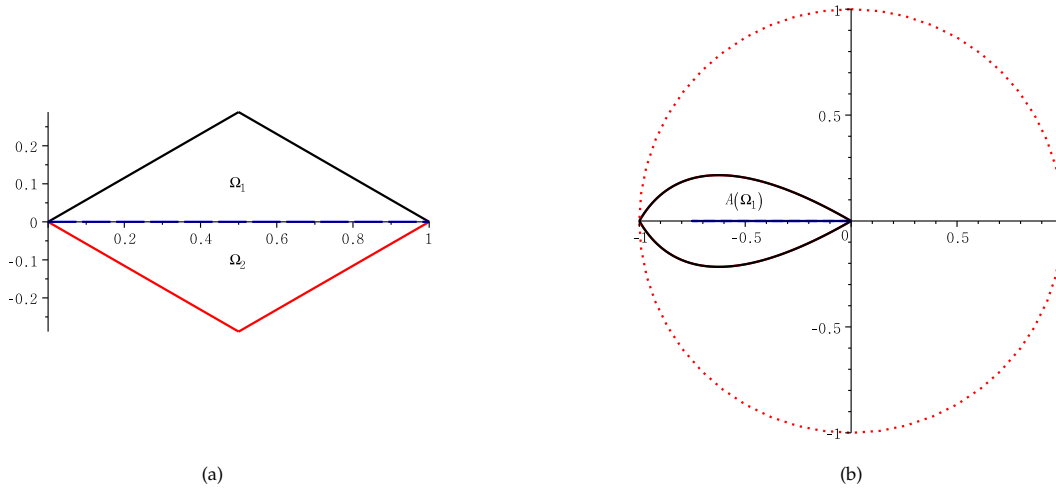(a)   (b)

Figure 1. (a) **c** belongs to $\Omega_1 \cup \Omega_2$ if and only if a PH cubic $\mathbf{r}(t) = \int_0^t \mathbf{k}(\tau - \mathbf{c})^2 d\tau + \mathbf{r}(0)$ has a loop.

(b) **c** $\in A(\Omega_1)$ if and only if a PH Möbius cubic has a loop

3. RPH curves on Enneper surfaces

In this section, we describe a PH preserving mapping on Enneper surfaces and construct a RPH curve from a C^1 Hermite date set.

Definition 3.1. *A mapping* **S** *is called a PH preserving mapping if for any RPH-curve* $\mathbf{r}(t)$, $\mathbf{S}(\mathbf{r}(t))$ *is a RPH curve. In particular, a mapping* $\mathbf{S}(u,v) = (x(u,v), y(u,v), z(u,v))$ *is called a scaled PH preserving mapping if, for any RPH curve* $\mathbf{r}(t) = (u(t), v(t))$, *there is a rational function* $P(u,v)$ *such that*

$$\| \alpha'(t) \|^2 = P(u,v)^2 \left(u'(t)^2 + v'(t)^2 \right),$$

where $\alpha(t) = \mathbf{S}(\mathbf{r}(t))$.

Lemma 3.2. ([9]) *Let* $\mathbf{S}(u,v) = (x(u,v), y(u,v), z(u,v))$ *be a mapping. Then* **S** *is scaled PH preserving if and only if*

$$\| \mathbf{S}_u(u,v) \|^2 = \| \mathbf{S}_v(u,v) \|^2 = P(u,v)^2,$$
$$< \mathbf{S}_u(u,v), \mathbf{S}_v(u,v) > = 0$$

for some rational function $P(u,v)$.

Now, we explain that an Enneper surface is one of scaled PH preserving mappings from the following example :

Example 3.3. Let $\mathbf{E} : \mathbb{R}^2 \to \mathbb{R}^3$ be an Enneper surface, given by

$$\mathbf{E}(u,v) = \left(\frac{u^3}{3} - uv^2 + u, \frac{v^3}{3} - vu^2 + v, 2uv \right).$$

Since $\|\mathbf{E}_u\|^2 = \|\mathbf{E}_v\|^2 = (u^2 + v^2 + 1)^2$ and $\langle \mathbf{E}_u, \mathbf{E}_v \rangle = 0$, the Enneper surface $\mathbf{E}(u,v)$ is a scaled PH preserving mapping (see Figure 2).

Definition 3.4. A C^1 Hermite data set $H_{C^1}^3 = \{\mathbf{P}_0, \mathbf{P}_1, \mathbf{V}_0, \mathbf{V}_1\}$, consisting of two end-points $\mathbf{P}_0$ and $\mathbf{P}_1$, and two velocities $\mathbf{V}_0$ and $\mathbf{V}_1$ at those end-points in $\mathbb{R}^3$, is said to be *regular* if $\mathbf{P}_1 - \mathbf{P}_0$, $\mathbf{V}_0$ and $\mathbf{V}_1$ are linearly independent. In particular, a regular C^1 Hermite data set

$$\{(0,0,0), \quad (1,0,0), \quad \mathbf{V}_0 = (v_{01}, v_{02}, 0), \quad \mathbf{V}_1 = (v_{11}, v_{12}, v_{13})\} \tag{3.1}$$

is called *the standard* C^1 *Hermite data set*, where $v_{02} \neq 0$ and $v_{13} \neq 0$, denoted by $\tilde{H}_{C^1}^3$.
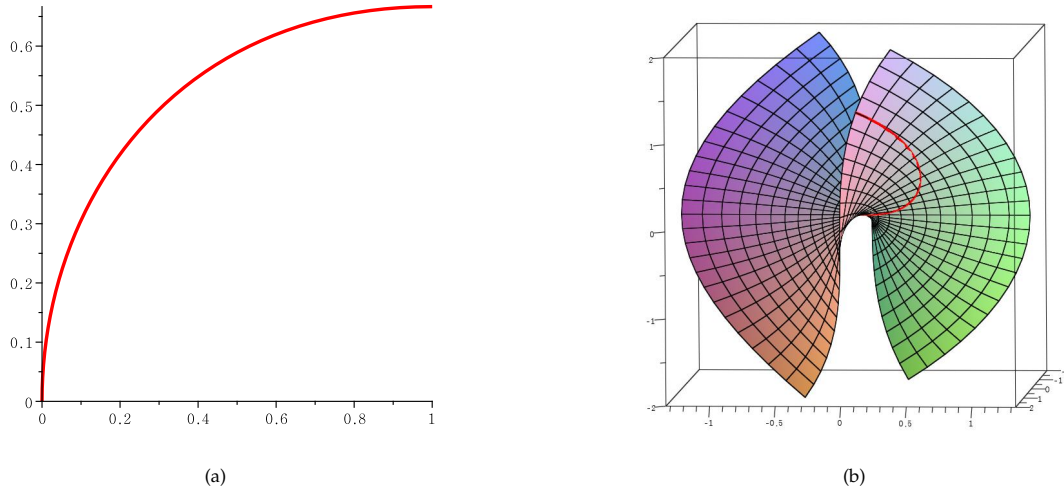
Figure 2. (a) $\mathbf{r}(t) = (t^2, \ t - \frac{1}{3}t^3)$ is a planar PH cubic.
(b) $\alpha(t) = \mathbf{E}(\mathbf{r}(t))$ is the PH curve on an Enneper surface.

Now, we describe a relation between a C^1 Hermite data set in $\mathbb{R}^2$ and a C^1 Hermite data set in $\mathbb{R}^3$ by using the Enneper surface $\mathbf{E}$.

Consider a RPH curve $\beta(t) = (u(t), v(t))$. Since the Enneper surface $\mathbf{E}$ is a scaled PH preserveing mapping, $\alpha(t) = \lambda \mathbf{E}(\beta(t))$ is a RPH curve with the standard C^1 Hermite data set $\tilde{H}^3_{C^1}$. On the other hand, we have

$$\alpha'(t) = \lambda u'(t)\mathbf{E}_u(\beta(t)) + \lambda v'(t)\mathbf{E}_v(\beta(t)). \tag{3.2}$$

Since $\mathbf{E}(0,0) = (0,0,0)$, $\mathbf{E}(u_0, 0) = (\frac{u_0^3}{3} + u_0, 0, 0)$, we can put $\beta(0) = (0,0)$ and $\beta(1) = (u_0, 0)$, which imply

$$\alpha(0) = \lambda \mathbf{E}(\beta(0)) = (0,0,0),$$

$$\alpha(1) = \lambda \mathbf{E}(\beta(1)) = \lambda(\frac{u_0^3}{3} + u_0, 0, 0).$$

We know that $\alpha(t)$ is a RPH curve with $\tilde{H}^3_{C^1}$, therefore $\alpha(1) = (1, 0, 0)$ and from the last equation we get

$$\lambda = \frac{3}{u_0^3 + 3u_0}. \tag{3.3}$$

Consequently, the following theorem characterizes a scaled Enneper surface, which is a PH preserving mapping, from a C^1 Hermite data set.

Theorem 3.5. *There exist two scaled Enneper surfaces with a given standard C^1 Hermite data set $\tilde{H}^3_{C^1}$.*

Proof. Let α be a curve on $\mathbb{R}^3$ satisfying the standard C^1 Hermite data set $\tilde{H}^3_{C^1}$ in (3.1). By (3.2), we get

$$\begin{aligned}
\alpha(0) &= \lambda \mathbf{E}(\beta(0)) = (0,0,0), \\
\alpha(1) &= \lambda \mathbf{E}(\beta(1)) = (1,0,0), \\
\alpha'(0) &= \lambda u'(0)\mathbf{E}_u(\beta(0)) + \lambda v'(0)\mathbf{E}_v(\beta(0)), \\
\alpha'(1) &= \lambda u'(1)\mathbf{E}_u(\beta(1)) + \lambda v'(1)\mathbf{E}_v(\beta(1)).
\end{aligned} \tag{3.4}$$

Since $\mathbf{E}_u(0,0) = (1,0,0)$ and $\mathbf{E}_v(0,0) = (0,1,0)$, the tangent plane of the Enneper surface at the origin is the xy−plane. Without loss of generality, we may assume $\beta(0) = (0,0)$ and $\beta(1) = (u_0, 0)$. By (3.4), we obtain

$u'(0) = \frac{v_{01}}{\lambda}$ and $v'(0) = \frac{v_{02}}{\lambda}$. Since $\mathbf{E}_u(u_0, 0) = \lambda(u_0^2 + 1, 0, 0)$ and $\mathbf{E}_v(u_0, 0) = \lambda(0, -u_0^2 + 1, 2u_0)$, it follows from (3.4) that one yields

$$\alpha'(1) = \lambda u'(1)(u_0^2 + 1, 0, 0) + \lambda v'(1)(0, -u_0^2 + 1, 2u) = (v_{11}, v_{12}, v_{13}).$$

Thus, we find

$$\begin{aligned} \lambda u'(1)(u_0^2 + 1) &= v_{11}, \\ \lambda v'(1)(-u_0^2 + 1) &= v_{12}, \\ 2u\lambda v'(1) &= v_{13}. \end{aligned} \tag{3.5}$$

Eliminating $\lambda v'(1)$ in (3.5) gives

$$v_{13}u_0^2 + 2v_{12}u_0 - v_{13} = 0,$$

which implies

$$u_0 = \frac{-v_{12} \pm \sqrt{v_{12}^2 + v_{13}^2}}{v_{13}}. \tag{3.6}$$

By (3.5), $u'(1) = \frac{v_{11}}{\lambda(u_0^2+1)}$ and $v'(1) = \frac{v_{13}}{2\lambda u_0^2}$. Also, from (3.4), we get $u'(0) = \frac{v_{01}}{\lambda}$ and $v'(0) = \frac{v_{02}}{\lambda}$. Thus, a set

$$\left\{ (0,0), \ (u_0, 0), \ \left(\frac{v_{01}}{\lambda}, \frac{v_{02}}{\lambda}\right), \ \left(\frac{v_{11}}{\lambda(u_0^2 + 1)}, \frac{v_{13}}{2\lambda u_0}\right) \right\} \tag{3.7}$$

is a C^1 Hermite data set of the RPH curve $\beta(t)$. Since the Enneper surface is a PH preserving mapping, the spatial curve $\alpha(t) = \lambda \mathbf{E}(\beta(t))$ is the RPH curve on the Enneper surface and there exist two scaled Enneper surfaces according to the real number u_0 in (3.6). This completes the proof. $\square$

Now, we explain the algorithm to construct spatial C^1 Hermite interpolation with a RPH curve on an Enneper surface.

Algorithm: spatial RPH curves on Enneper surfaces

Input: The standard C^1 Hermite data set $\tilde{H}_{C^1}^3$.

1. Compute u_0 by (3.6) and λ by (3.3).

2. Find the planar C^1 Hermite data set $H_{C^1}^2$ by (3.7).

3. Represent the set $H_{C^1}^2$ on a complex plane.

4. Find the standard C^1 Hermite data set $\tilde{H}_{C^1}^2$ by scaling $\frac{1}{u_0}$ at $H_{C^1}^2$.

5. Solve PH Möbius cubic interpolants satisfying the set $\tilde{H}_{C^1}^2$.

6. Find a planar RPH curve $\beta(t)$, multiplying u_0 by the PH Möbius cubics.

Output: The spatial RPH curve $\alpha(t) = \lambda \mathbf{E}(\beta(t))$ satisfying the set $\tilde{H}_{C^1}^3$.

Example 3.6. Consider the standard C^1 Hermite data set $\tilde{H}_{C^1}^3 = \{(0,0,0), (1,0,0), \mathbf{V}_0, \mathbf{V}_1\}$ given by $\mathbf{V}_0 = (1, 2, 0)$ and $\mathbf{V}_1 = (2, 1, 2)$. Then, from (3.6) we can obtain $u_0 = \frac{-1+\sqrt{5}}{2}$ or $\frac{-1-\sqrt{5}}{2}$, that is, there exist two scaled Enneper surfaces for a spatial PH curve satisfying $\tilde{H}_{C^1}^3$

1. Case $u_0 = \frac{-1+\sqrt{5}}{2}$: In this case we obtain $\lambda = \frac{21+15\sqrt{5}}{38}$ and the planar C^1 Hermite data set

$$H_{C^1}^2 = \{(0,0), \, (\frac{-1+\sqrt{5}}{2}, 0), (\frac{-7+5\sqrt{5}}{6}, \frac{-7+5\sqrt{5}}{3}), (\frac{-5+9\sqrt{5}}{15}, \frac{9-\sqrt{5}}{6})\}.$$

By process of the algorithm, we obtain the four PH Möbius cubics $\beta(t)$ satisfying the standard C^1 Hermite data set
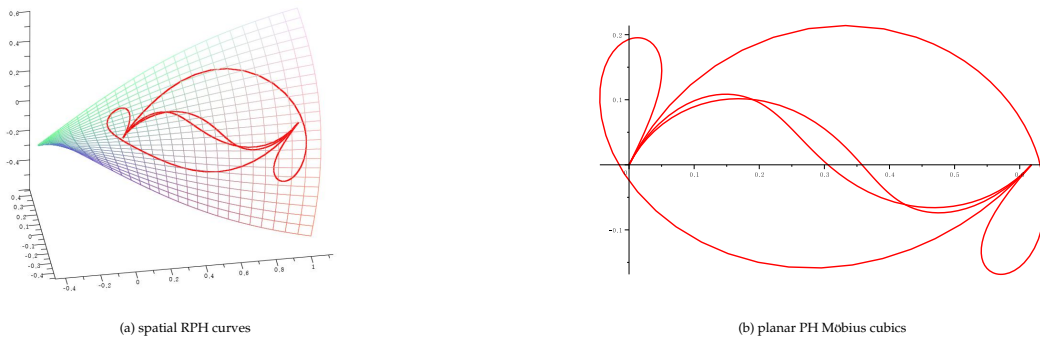
$$\tilde{H}_{C^1}^2 = \{0, 1, \frac{9-\sqrt{5}}{6} + \frac{9-\sqrt{5}}{3}i, \frac{20+2\sqrt{5}}{15} + \frac{1+2\sqrt{5}}{3}i\}$$

on a complex plane. Thus, we have the four spatial RPH curves $\alpha(t) = \lambda \mathbf{E}(\beta(t))$ satisfying $\tilde{H}_{C^1}^3$ on the Enneper surface with the help of the PH Möbius cubic $\beta(t)$ and the scaled PH preserving mapping $\mathbf{E}$ as Figure 3.

2. Case $u_0 = \frac{-1-\sqrt{5}}{2}$: In this case we have $\lambda = \frac{21-15\sqrt{5}}{38}$ and the planar C^1 Hermite data set $H_{C^1}^2 = \{(0,0), \, (\frac{-1-\sqrt{5}}{2}, 0), (\frac{-7-5\sqrt{5}}{6}, \frac{-7-5\sqrt{5}}{3}), (\frac{-5-9\sqrt{5}}{15}, \frac{9+\sqrt{5}}{6})\}$. By process of the algorithm we find the four PH Möbius cubics $\beta(t)$ satisfying the standard C^1 Hermite data set

$$\tilde{H}_{C^1}^2 = \{0, 1, \frac{9+\sqrt{5}}{6} + \frac{9+\sqrt{5}}{3}i, \frac{20-2\sqrt{5}}{15} + \frac{1-2\sqrt{5}}{3}i\}$$

on a complex plane. It follows that we can find the four spatial RPH interpolants $\alpha(t) = \lambda \mathbf{E}(\beta(t))$ satisfying the set $\tilde{H}_{C^1}^3$ on the Enneper surface as Figure 4.
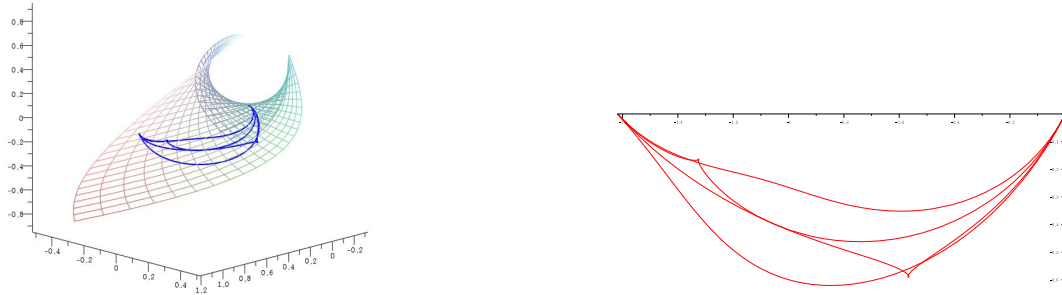

(a) spatial RPH curves

(b) planar PH Möbius cubics

Figure 3. Case $u_0 = \frac{-1+\sqrt{5}}{2}$: (a) is four RPH curves on Enneper surface satisfying
$\tilde{H}_{C^1}^3 = \{(0,0,0), (1,0,0), \mathbf{V}_0 = (1,2,0), \mathbf{V}_1 = (2,1,2)\}$. (b) is four PH Möbius cubics satisfying
the standard C^1 Hermite data set $\tilde{H}_{C^1}^2 = \{0, 1, \frac{9-\sqrt{5}}{6} + \frac{9-\sqrt{5}}{3}i, \frac{20+2\sqrt{5}}{15} + \frac{1+2\sqrt{5}}{3}i\}$

In Example 3.6, for the given set $\tilde{H}_{C^1}^3$ we explain C^1 Hermite interpolation by using scaled Enneper surfaces and PH Möbius cubics. Next, we describe a C^1 Hermite interpolation with a C^1 Hermite data set $H_{C^1}^3$ in Example 3.7. We add the process to convert a given $H_{C^1}^3$ into $\tilde{H}_{C^1}^3$ by using an orthogonal transformation.

(a) spatial RPH curves
(b) planar PH Möbius cubics

Figure 4. Case $u_0 = \frac{-1-\sqrt{5}}{2}$: (a) is four RPH curves on Enneper surface satisfying the standard C^1 Hermite data set $\tilde{H}^3_{C^1} = \{(0,0,0), (1,0,0), \mathbf{V}_0 = (1,2,0), \mathbf{V}_1 = (2,1,2)\}$. (b) is four PH Möbius cubics satisfying $\tilde{H}^2_{C^1} = \{0, 1, \frac{9+\sqrt{5}}{6} + \frac{9+\sqrt{5}}{3} i, \frac{20-2\sqrt{5}}{15} + \frac{1-2\sqrt{5}}{3} i\}$

Example 3.7. Consider a C^1 Hermite data set $H^3_{C^1} = \{\mathbf{P}_0, \mathbf{P}_1, \mathbf{V}_0, \mathbf{V}_1\}$ with $\mathbf{P}_0 = (0,0,0)$, $\mathbf{P}_1 = (1,1,1)$, $\mathbf{V}_0 = (0,1,1)$ and $\mathbf{V}_1 = (2,1,2)$. Let a set $\{\mathbf{F}_1, \mathbf{F}_2, \mathbf{F}_3\}$ be an orthogonal basis determined by $\mathbf{F}_1 = \frac{\mathbf{P}_1-\mathbf{P}_0}{\|\mathbf{P}_1-\mathbf{P}_0\|}$, $\mathbf{F}_3 = \frac{\mathbf{F}_1 \times \mathbf{V}_0}{\|\mathbf{F}_1 \times \mathbf{V}_0\|}$ and $\mathbf{F}_2 = \mathbf{F}_3 \times \mathbf{F}_1$. Then, there exists the orthogonal matrix $\mathbf{M} \in O(3)$ given by

$$\mathbf{M} = \begin{pmatrix} \frac{\sqrt{3}}{3} & -\frac{\sqrt{6}}{3} & 0 \\ \frac{\sqrt{3}}{3} & \frac{\sqrt{6}}{6} & -\frac{\sqrt{2}}{2} \\ \frac{\sqrt{3}}{3} & \frac{\sqrt{6}}{6} & \frac{\sqrt{2}}{2} \end{pmatrix},$$

via $\mathbf{MF}_1 = (1,0,0)$, $\mathbf{MF}_2 = (0,1,0)$ and $\mathbf{MF}_3 = (0,0,1)$ as the matrix multiplication $\mathbf{MF}_i (i = 1,2,3)$. By using the orthogonal matrix $\mathbf{M}$, we can obtain the standard C^1 Hermite data set

$$\tilde{H}^3_{C^1} = \{\mathbf{MP}_0 = (0,0,0), \mathbf{MP}_1 = (1,0,0), \tilde{\mathbf{V}}_0 = \mathbf{MV}_0, \tilde{\mathbf{V}}_1 = \mathbf{MV}_1\}.$$

Using the algorithm, one find the RPH curve $\tilde{\alpha}(t) = \lambda \mathbf{E}(\beta(t))$ satisfying $\tilde{H}^3_{C^1}$. Thus, we conclude that the RPH curves $\alpha(t) = \mathbf{M}^{-1}(\tilde{\alpha}(t))$ are interpolants satisfying given the C^1 Hermite data set $H^3_{C^1}$ and we have the picture shown in Figure 5.
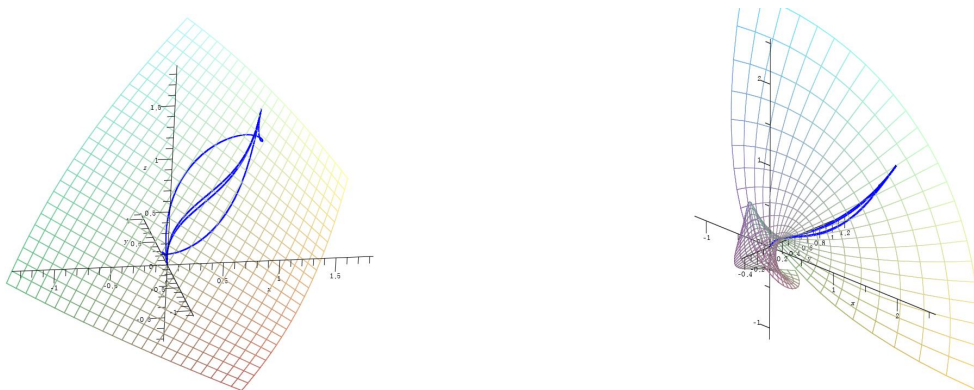
(a) RPH curves of case $u_0 > 0$
(b) RPH curves of case $u_0 < 0$

Figure 5. (a) and (b) are RPH curves on two Enneper surfaces satisfying the C^1 Hermite data set $H^3_{C^1}$.

Next, we consider a bending energy $\mathcal{E}$ of a curve as

$$\mathcal{E}(\gamma) = \int_{\gamma} \kappa^2 \, ds,$$

where κ is the curvature of an interpolant γ. The bending energy $\mathcal{E}$ of a curve is an established measure of its fairness. We can explain an interpolant to have a better shape than another if it has lower bending energy with a similar arc-length as the following table.

$u_0 = \frac{-1+\sqrt{5}}{2}$	RPH_1	RPH_2	RPH_3	RPH_4	MC_1	MC_2	MC_3	MC_4
arc-length	1.19	1.19	1.86	2.16	0.74	0.74	1.19	1.22
BE	14.52	14.35	53.31	46.34	20.21	20.65	74.57	86.43

$u_0 = \frac{-1-\sqrt{5}}{2}$	RPH_1	RPH_2	RPH_3	RPH_4	MC_1	MC_2	MC_3	MC_4
arc-length	1.28	1.34	1.16	1.47	1.96	2.06	1.83	2.13
BE	4393	3328	13.18	13.70	4023	1828	2.94	2.66

Table 1: Comparison of arc-length and bending energy for the interpolants of Figure 4 and Figure 5

4. Conclusions

Representations of curves and surfaces given by polynomial or rational parameterizations are very important for computer aided design. In this work, we show that a parametrization of the Enneper surface is PH-preserving, and there are two scaled Enneper surfaces satisfying any regular C^1 Hermite data set. As a result, we construct spatial RPH curves satisfying the C^1 Hermite data set on the Enneper surfaces. Moreover, we introduce how to compute the bending energy for curves on the surface in order to choose better curves as well as we analyze arc length and bending energy through examples.

References

[1] R. Ait-Haddou, W. Herzog, L. Biard, *Pythagorean-hodograph ovals of constant width*, Comput. Aided Geom. Design **25** (2008), 258–273.
[2] M. Bizzarri, M. Lávička, J. Vršek, *Linear computational approach to interpolations with polynomial Minkowski Pythagorean hodograph curves*, J. Comput. Appl. Math. **361** (2019), 283–294.
[3] M. M. Byrtus, *Parametrization methods of algebraic varieties*, A thesis for the degree of Doctor of Philosophy, University of West Bohemia, 2011.
[4] C. Cetin, I. Kazim, *A new method for construction of PH-helical curves in* $\mathbb{E}^3$, C. R. Acad. Bulgare Sci. **72** (2019), 301–308.
[5] H. I. Choi, S. W. Choi, C. Y. Han, H. P. Moon, "*Mathematical theory of medial axis transform*, Pacific J. Math. **181** (1997), 57 – 88.
[6] R. T. Farouki, T. Sakkalis, *Pythagorean hodographs*, IBM J. Res. Develop. **34** (1990), 736 – 752.
[7] Z. Habib, M. Sakai, G^2 *Pythagorean quintic transition between two circles with shape control*, Comput. Aided Geom. Design **24** (2007), 252 – 266.
[8] K. Jernej, K. Marjeta, V. Vito, *Dual representation of spatial rational Pythagorean-hodograph curves*, Comput. Aided Geom. Design **31** (2014), 43–56.
[9] G. Kim, S. Lee, *Pythagorean-hodograph preserving mappings*, J. Comput. Appl. Math. **216** (2008), 217 – 226.
[10] J. H. Kong, S. Lee, G. Kim, *Minkowski Pythagorean-hodograph preserving mappings*, J. Comput. Appl. Math. **308** (2016), 166 – 176.
[11] J. Kosinka, B. Jüttler, C^1 *Hermite interpolation by Pythagorean hodograph quintics in Minkowski space*, Adv. Comput. Math. **30** (2009), 123 – 140.
[12] S. Lee, H. C. Lee, M. R. Lee, S. Jeong, G. I. Kim, *Hermite interpolation using Möbius transformations of planar Pythagorean-hodograph cubics*, Abstr. Appl. Anal. Article ID 560246 (2012), 1 – 15.
[13] H. C. Lee, J. W. Lee, D. W. Yoon, *Interpolation of surfaces with geodesic*, J. Korean Math. Soc. **57** (2020), 957–971.
[14] K. Marjeta, *Interpolation with spatial rational Pythagorean-hodograph curves of class 4*, Comput. Aided Geom. Design **56** (2017), 16–34.
[15] H. P. Moon, *Minkowski Pythagorean hodographs*, Comput. Aided Geom. Design **16** (1999), 739 – 753.
[16] H. Pottmann, *Rational curves and surfaces with rational offsets*, Comput. Aided Geom. Design **12** (1995), 175 – 192.
[17] A. Sestini, L. Landolfi, C. Manni, *On the approximation order of a space data-dependent PH quintic Hermite interpolation scheme*, Comput. Aided Geom. Design **30** (2013), 148 – 158 .
[18] D. J. Walton, D. S. Meek, *Geometric Hermite interpolation with Tschirnhausen cubics*, J. Comput. Appl. Math. **81** (1997), 299 – 309.